Large Area of Ultraviolet GaN-Based Photonic Quasicrystal Laser

2012 Jpn. J. Appl. Phys. 51 04DG02

(http://iopscience.iop.org/1347-4065/51/4S/04DG02)

DOI: 10.1143/JJAP.51.04DG02

Large Area of Ultraviolet GaN-Based Photonic Quasicrystal Laser

Cheng-Chang Chen[1], Ching-Hsueh Chiu[1], Po-Min Tu[1], Ming-Yen Kuo[2], M. H. Shih[1,2*],
Ji-Kai Huang[1], Hao-Chung Kuo[1], Hsiao-Wen Zan[1], and Chun-Yen Chang[3]

[1] *Department of Photonics & Institute of Electro-Optical Engineering, National Chiao Tung University, Hsinchu 300, Taiwan, R.O.C.*
[2] *Research Center for Applied Sciences (RCAS), Academia Sinica, Nankang, Taipei 115, Taiwan, R.O.C.*
[3] *Department of Electronics Engineering National Chiao Tung University, Hsinchu 30010, Taiwan, R.O.C.*

Received September 26, 2011; accepted January 26, 2012; published online April 20, 2012

In this study, large-area GaN-based photonic quasicrystal (PQC) nanopillars were fabricated on an n-GaN substrate using the nanoimprint lithography (NIL) technique. Under optical pumping condition, a high lasing action from the GaN photonic quasicrystals was observed. The lasing wavelength is at 366 nm with a low threshold power density of 0.009 kW/cm^2. To confirm the band-edge lasing mode, the finite-element method (FEM) was used to perform the simulation for the 12-fold symmetry photonic quasicrystal lattices.

1. Introduction

The wide and direct band gap of GaN-based materials has been attracting much attention for applications such as light-emitting diodes (LEDs) and laser diodes (LDs).[1–5] The high-brightness GaN-based LEDs have been applied in traffic signals, backlights in liquid crystal displays, and solid state lighting.[6] The blue LD can serve as the light source of high density data storage in a high-definition digital versatile disk (HD-DVD), which is one of the popular data storage tools. Nevertheless, for applications, the high extraction efficiency of the light source needs to be improved and promoted. In general, there are several methods to increase the light extraction efficiency of GaN-based LEDs such as surface roughness,[7,8] photon recycling technique,[9,10] and the use of photonic crystal structures.[11,12] In the latter method, the photonic crystal structure has a periodic structure with translational symmetry. The periodic structure can exhibit the photonic band gap (PBG) to inhibit the propagation of guided modes[13] and utilize the photonic crystal structure to couple guided modes to radiative modes.[14–16] There are reports on photonic crystal lasers of utilizing photonic crystal band-edge modes.[17–19] Most of the reported photonic crystal structures were fabricated by E-beam lithography[20] or laser interference lithography.[21] However, compared the two methods mentioned above to nanoimprint lithography (NIL), NIL is suitable for the mass production of LED devices owing to its good resolution and higher throughput with low fabrication cost. In this study, we demonstrated a GaN-based two-dimensional (2D) photonic quasicrystal (PQC) structure as shown in Fig. 1. The fabrication of a PQC structure is used for the nanoimprint lithography (NIL).[22] The photonic quasicrystal structures possess 12-fold symmetry[22,23] and form a complete band gap. Under room temperature pulse operation, experimental results reveal that the device has lasing action with a low threshold power density.

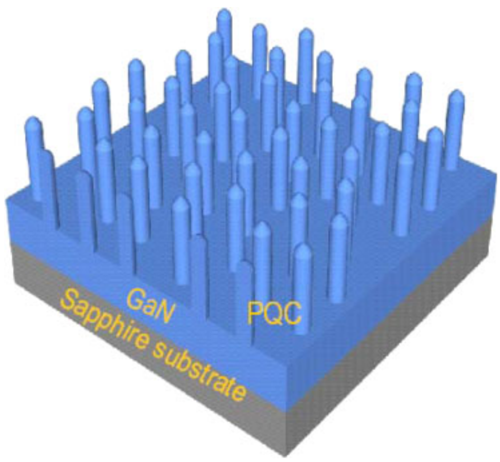

Fig. 1. (Color online) Schematic diagram of GaN-based PQC structure on sapphire substrate.

2. Fabrication Process

The fabrication procedures of the GaN QPC structure include epitaxial growth of a GaN wafer, nanoimprint lithography of QPC patterns, and the dry etching step. The GaN-based material was grown using a low pressure metal–organic chemical vapor deposition (MOCVD) system on 2-in. diameter (0001)-oriented sapphire substrates using trimethylgallium and trimethylaluminum as group III source materials and ammonia as the group V source material. A 2-μm-thick GaN was first grown on a 2-in. *C*-plane (0001) sapphire substrate. The GaN contained 1 μm undoped GaN and 1 μm n-type GaN and were grown at 1150 and 1160 °C, respectively. The PQC lattices were formed by NIL with a 2-in. PQC mold. First, a 400 nm SiO_2 layer and a 200 nm polymer layer were deposited as the masks during the process. Then, a patterned mold of PQC structure was placed onto the dried polymer film. By applying a high pressure, the substrate was heated to above the glass transition temperature of the polymer. After that, the substrate and mold were cooled to room temperature to release the mold. The PQC patterns were defined on the polymer layer and the patterns were then transferred into a SiO_2 layer by reactive ion etching (RIE) with a CHF_3/O_2 mixture. The structure was then etched by inductively coupled plasma reactive ion etching (ICP-RIE) with a Cl_2/Ar mixture. The mask layers were removed at the end of the processes. The detailed fabrication process of NIL flow is shown in Fig. 2. For this study, the size of the fabricated GaN PQC structure is approximately 1 cm^2. The PQC structure has a lattice constant (a) of 460 nm, a diameter (r) of 160 nm, and a height of 1 μm. Figure 3 shows the fabricated GaN PQC sample (a) and its scanning electron microscopy (SEM) images from (b) the top view and (c) the angle view.

*E-mail address: mhshih@gate.sinica.edu.tw

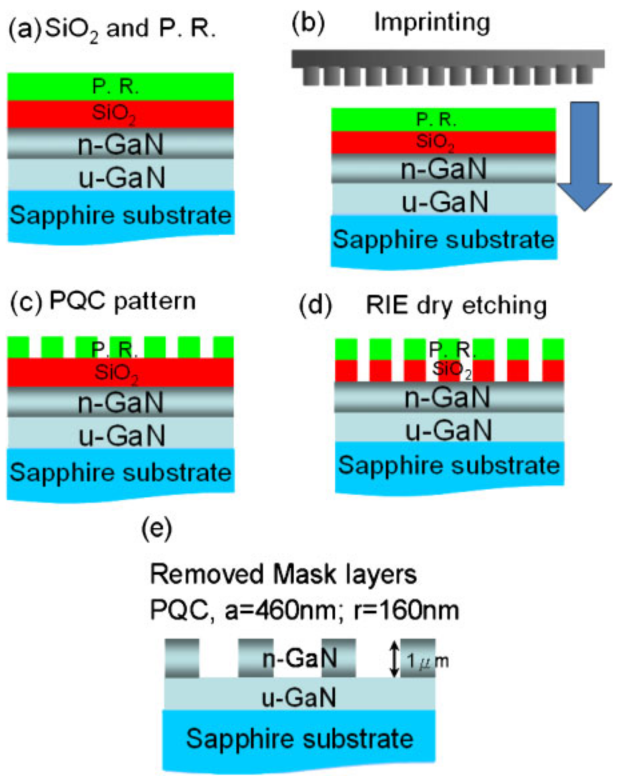

Fig. 2. (Color online) Illustrations of fabrication process of nanoimprint technology. (a) SiO_2 and polymer were deposited. (b) Pattern mold of PQC structure was placed onto the polymer layer. (c) PQC pattern was defined on the polymer layer. (d) RIE dry etching process. (e) Photonic quasicrystal pattern was fabricated on epitaxial structure.

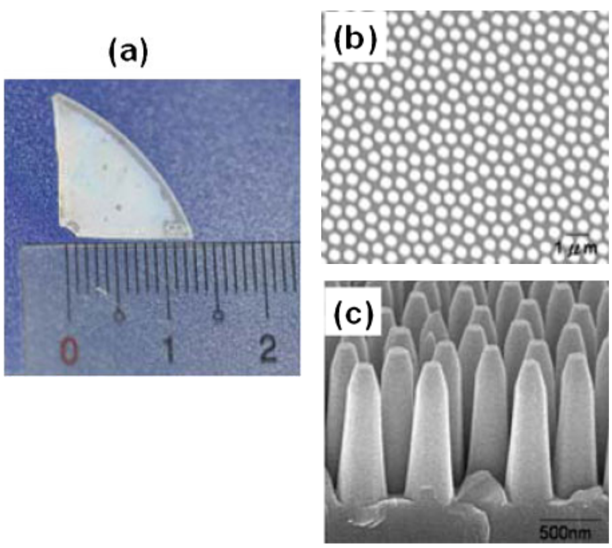

Fig. 3. (Color online) (a) Image of fabricated GaN PQC sample. SEM images of the PQC structure from (b) the top-view and (c) the angle-view.

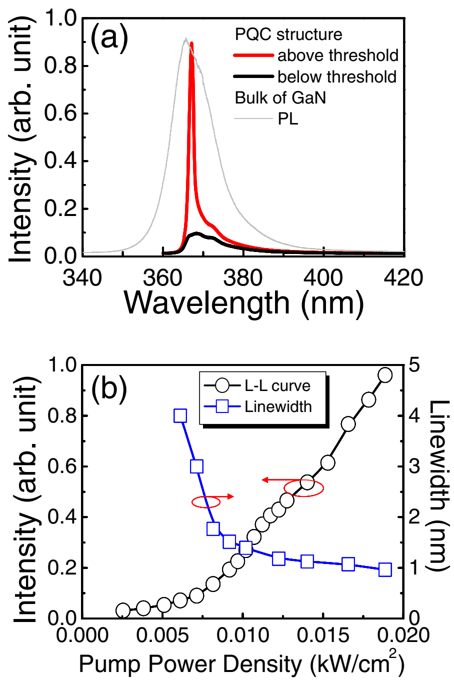

Fig. 4. (Color online) (a) Measured spectrum of the PQC laser below (black) and above (red) threshold, and the photoluminescence (gray curve) of bulk GaN. The lasing wavelength of the PQC is 366 nm. (b) The light-in and light-out (L–L) curve and linewidth narrowing.

3. Measurement and Discussion

To demonstrate the lasing action from the photonic quasicrystal structure, optical pumping was performed by using a frequency-tripled Nd:YVO_4 355 nm pulsed laser with a pulse width of 0.5 ns and a repetition rate of 1 kHz. The device was pumped by a normal incident laser beam with a spot size of 50 μm. The light emission from the sample was collected by a 15× objective lens through a multimode fiber, and coupled into a spectrometer with a charge-coupled device (CCD). Under room-temperature optical pumping condition, a strong lasing emission from the photonic quasicrystal pattern was observed, as shown in Fig. 4. Figure 4(a) shows the measured spectra from the PQC pattern below (black curve) and above (red curve) the threshold, and the photoluminescence (PL) (gray curve) of bulk GaN with a bandwidth of 15 nm. Obviously, the lasing action was observed at 366 nm wavelength with the bandwidth of 1 nm due to the distributed feedback of light at the photonic band edge of the PQC structure.[23,24] The light-in and light-out (L–L) curve and the linewidth narrowing are shown in Fig. 4(b). The threshold power density was observed at approximately 0.009 kW/cm^2. This value corresponds to a threshold energy density of 9 mJ/cm^2, which is reasonable in comparison with the reported GaN threshold gain (~1.1 mJ/cm^2).[25] This ultralow threshold also indicates the strong enhancement from photonic quasicrystal lattices. The quality factor of the QPC structure is approximately 350, which is estimated from the ratio of the lasing wavelength to the linewidth around the transparency (i.e., $Q \sim \lambda/\Delta\lambda$). The observed signal-to-background ratio of the lasing is approximately 9 dB at 1.5 times the threshold. This is because of the limited pump power density and the background PL signal from the bottom GaN layer.

4. Simulation and Analysis

To understand the lasing mode, we used the finite-element method (FEM)[26] to calculate the transmission spectrum[27] of the PQC with the incident angles of 0, 5, 10, 15, 20, and 25°, as shown in Fig. 5(a). Owing to the symmetry of this PQC,

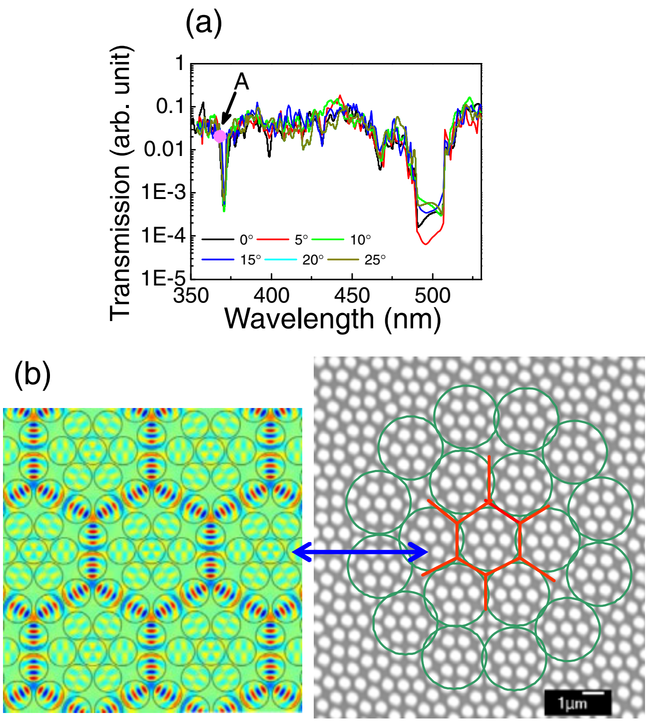

Fig. 5. (Color online) (a) Corresponding transmission spectrum was calculated by FEM method. (b) Electric-field distribution was also calculated by FEM simulation.

the spectra will repeat for every 30° incident angle. Therefore we can confirm the photonic band gaps from the calculated spectra. By comparing the experimental simulation and data, the observed lasing mode corresponds to the normalized frequency as $a/\lambda \sim 1.25$ (circular point) around the band edge, which is labeled as mode A. Figure 5(b) shows the calculated mode profile of the mode A, which indicates the high symmetry of this operated mode in the PQC structure. It is worth noting that the band-edge lasing of the GaN PQC with a 460 nm lattice constant was designed to work around the higher frequency band gap. This is because the fabrication of the large-area GaN PQC structure with a smaller lattice constant is relatively difficult.

5. Conclusions

In short, a 12-fold symmetric GaN PQC nanopillar structure was fabricated using NIL. The UV lasing action was observed at approximately 366 nm wavelength with an ultralow threshold power density of $0.009\,\mathrm{kW/cm^2}$. To check the lasing mode is the band edge mode. The optical mode profile of the lasing mode was characterized with FEM simulation, and the experimental results show excellent agreement with the simulations. The NIL fabrication procedure demonstrated has high potential to resulting in a low fabrication cost. Owing to the larger emission area, lower threshold power and lower fabrication cost of the device, we believe that the large area photonic quasicrystal laser could be one of potential light sources for future integration circuit applications.

Acknowledgements

The authors are grateful to the National Chiao Tung University's Center for Nano Science and Technology, National Nano Device Laboratories (NDL), and the National Science Council of the Republic of China, Taiwan, for financially supporting this research under Contract nos. NSC 99-2112-M-001-033-MY3 and NSC98-3114-E009-002-CC2.

1) S. Nakaira, T. Mukai, and M. Senoh: Appl. Phys. Lett. **64** (1994) 1687.
2) S. Nakamura, M. Senoh, N. Iwasa, and S. Nagahama: Jpn. J. Appl. Phys. **34** (1995) L797.
3) S. Nakamura, M. Senoh, S. Nagahama, N. Iwasa, T. Yamada, T. Matsushita, Y. Sugimoto, and H. Kiyoku: Appl. Phys. Lett. **70** (1997) 868.
4) S. Nakamura: Science **281** (1998) 956.
5) E. D. Haberer, R. Sharma, C. Meier, A. R. Stonas, S. Nakamura, S. P. DenBaars, and E. L. Hu: Appl. Phys. Lett. **85** (1997) 5179.
6) M. Koike, N. Shibata, H. Kato, and Y. Takahashi: IEEE J. Sel. Top. Quantum Electron. **8** (2002) 271.
7) T. Fujii, Y. Gao, R. Sharma, E. L. Hu, S. P. DenBaars, and S. Nakamura: Appl. Phys. Lett. **84** (2004) 855.
8) R. H. Horng, C. C. Yang, J. Y. Wu, S. H. Huang, C. E. Lee, and D. S. Wuu: Appl. Phys. Lett. **86** (2005) 221101.
9) V. V. Nikolaev, M. E. Portnoi, and I. Eliashevich: Phys. Status Solidi A **183** (2001) 177.
10) H. De Neve, J. Blondelle, P. Van Daele, P. Demeester, R. Baets, and G. Borghs: Appl. Phys. Lett. **70** (1997) 799.
11) J. Shakya, K. H. Kim, J. Y. Lin, and H. X. Jiang: Appl. Phys. Lett. **85** (2004) 142.
12) J. J. Wierer, M. R. Krames, J. E. Epler, N. F. Gardner, M. G. Craford, J. R. Wendt, J. A. Simmons, and M. M. Sigalas: Appl. Phys. Lett. **84** (2004) 3885.
13) M. Boroditsky, T. F. Krauss, R. Coccioli, R. Vrijen, R. Bhat, and E. Yablonovitch: Appl. Phys. Lett. **75** (1999) 1036.
14) M. Rattier, H. Benisty, E. Schwoob, C. Weisbuch, T. F. Krauss, C. J. M. Smith, R. Houdre, and U. Oesterle: Appl. Phys. Lett. **83** (2003) 1283.
15) D. Delbeke, P. Bienstman, R. Bockstaele, and R. Baets: J. Opt. Soc. Am. A **19** (2002) 871.
16) A. David, T. Fujii, R. Sharma, K. McGroddy, S. Nakamura, S. P. DenBaars, E. L. Hu, C. Weisbuch, and H. Benisty: Appl. Phys. Lett. **88** (2006) 061124.
17) H. Matsubara, S. Yoshimoto, H. Saito, Y. Jianglin, Y. Tanaka, and S. Noda: Science **319** (2008) 445.
18) S. Noda, M. Yokoyama, M. Imada, A. Chutinan, and M. Mochizuki: Science **293** (2001) 1123.
19) S. W. Chen, T. C. Lu, Y. J. Hou, T. C. Liu, H. C. Kuo, and S. C. Wang: Appl. Phys. Lett. **96** (2010) 071108.
20) H. Yu, J. Yu, F. Sun, Z. Li, and S. Chen: Opt. Commun. **271** (2007) 241.
21) L. Vogelaar, W. Nijdam, H. A. G. M. van Wolferen, R. M. de Ridder, F. B. Segerink, E. Flück, L. Kuipers, and N. F. van Hulst: Adv. Mater. **13** (2001) 1551.
22) H. W. Huang, C. H. Lin, K. Y. Lee, C. C. Yu, J. K. Huang, B. D. Lee, H. C. Kuo, K. M. Leung, and S. C. Wang: Semicond. Sci. Technol. **24** (2009) 085008.
23) M. E. Zoorob, M. D. B. Charlton, G. J. Parker, J. J. Baumberg, and M. C. Netti: Nature (London) **404** (2000) 740.
24) K. Nozaki and T. Baba: Jpn. J. Appl. Phys. **45** (2006) 6087.
25) S. Juršenas, N. Kurilèik, G. Kurilèik, S. Miasojedovas, A. Žukauskas, T. Suski, P. Perlin, M. Leszczynski, P. Prystawko, and I. Grzegory: Appl. Phys. Lett. **85** (2004) 952.
26) W. J. Kim and J. D. O'Brien: J. Opt. Soc. Am. B **21** (2004) 289H.
27) H. Zhao, R. P. Zaccaria, J. F. Song, S. Kawata, and H. B. Sun: Phys. Rev. B **79** (2009) 115118.